TISSUE ENGINEERING: Part A
Volume 27, Numbers 13 and 14, 2021

DOI: 10.1089/ten.tea.2020.0135

termis
Tissue Engineering
& Regenerative Medicine
International Society

ORIGINAL ARTICLE

Cerebellar Differentiation from Human Stem Cells Through Retinoid, Wnt, and Sonic Hedgehog Pathways

Thien (Timothy) Hua, MS,[1] Julie Bejoy, PhD,[2,*] Liqing Song, PhD,[2,†] Zhe Wang, MS,[1] Ziwei Zeng, MS,[1,3] Yi Zhou, PhD,[4] Yan Li, PhD,[2,5] and Qing-Xiang Amy Sang, PhD[1,5]

Differentiating cerebellar organoids can be challenging due to complex cell organization and structure in the cerebellum. Different approaches were investigated to recapitulate differentiation process of the cerebellum from human-induced pluripotent stem cells (hiPSCs) without high efficiency. This study was carried out to test the hypothesis that the combination of different signaling factors including retinoic acid (RA), Wnt activator, and sonic hedgehog (SHH) activator promotes the cerebellar differentiation of hiPSCs. Wnt, RA, and SHH pathways were activated by CHIR99021 (CHIR), RA, and purmorphamine (PMR), respectively. Different combinations of the morphogens (RA/CHIR, RA/PMR, CHIR/PMR, and RA/CHIR/PMR) were utilized, and the spheroids (day 35) were characterized for the markers of three cerebellum layers (the molecular layer, the Purkinje cell layer, and the granule cell layer). Of all the combinations tested, RA/CHIR/PMR promoted both the Purkinje cell layer and the granule cell layer differentiation. The cells also exhibited electrophysiological characteristics using whole-cell patch clamp recording, especially demonstrating Purkinje cell electrophysiology. This study should advance the understanding of different signaling pathways during cerebellar development to engineer cerebellum organoids for drug screening and disease modeling.

Keywords: induced pluripotent stem cells, cerebellum, spheroids, Wnt, sonic hedgehog, retinoic acid

Impact Statement

This study investigated the synergistic effects of retinoic acid, Wnt activator, and sonic hedgehog activator on cerebellar patterning of human-induced pluripotent stem cell (hiPSC) spheroids and organoids. The results indicate that the combination promotes the differentiation of the Purkinje cell layer and the granule cell layer. The cells also exhibit electrophysiological characteristics using whole-cell patch clamp recording, especially demonstrating Purkinje cell electrophysiology. The findings are significant for understanding the biochemical signaling of three-dimensional microenvironment on neural patterning of hiPSCs for applications in organoid engineering, disease modeling, and drug screening.

Introduction

Human-induced pluripotent stem cells (hiPSCs) can generate organoids that have patterns and functions similar to human tissues,[1] and can be used to model and understand human tissue development and disease progression.[2,3] Generating spheroids or organoids that mimic different human brain regions, including forebrain, midbrain, hindbrain, and the spinal cord, from hiPSCs *in vitro* has been reported recently.[4–9] Cerebellum is located in the hindbrain region and consists of high density and complexity of neurons in the human brain.[10] Thus it is challenging to differentiate cerebellar-like organoids with similar cellular markers and organization to the human brain. To date, few studies have been reported to generate cerebellar-like organoids from hiPSCs.

[1]Department of Chemistry and Biochemistry, Florida State University, Tallahassee, Florida, USA.
[2]Department of Chemical and Biomedical Engineering, FAMU-FSU College of Engineering, Florida State University, Tallahassee, Florida, USA.
[3]Department of Colorectal Surgery, the Sixth Affiliated Hospital of Sun Yat-sen University, Guangzhou, People's Republic of China.
[4]Department of Biomedical Sciences, College of Medicine, Florida State University, Tallahassee, Florida, USA.
[5]Institute of Molecular Biophysics, Florida State University, Tallahassee, Florida, USA.
**Current affiliation:* College of Medicine, Vanderbilt University, Nashville, Tennessee, USA.
[†]*Current affiliation:* Department of Chemical Engineering, Carnegie Mellon University, Pittsburgh, Pennsylvania, USA.

The approaches to differentiate cerebellar spheroids or organoids are based on the events of embryonic development. By regulating the patterning signal gradients, hiPSCs can differentiate into specific subtypes of neural cells along the anterior–posterior (A-P) and dorsal–ventral (D-V) axes of the brain.[11] First, the formation of the isthmic organizer acts as a midbrain–hindbrain boundary that creates a feedback loop of fibroblast growth factor (FGF) 8 and Wnt ligands to govern the anterior–posterior pattern of the caudal midbrain–rostral hindbrain and maintain isthmic identity.[12] The cerebellum anlage is developed in the dorsal region of the rostral hindbrain, specifically at the alar plate of the rhombomere 1 (rh1).[13–15] Two distinct germinal zones in rh1, the ventricular zone (VZ) and the rhombic lip, give rise to cerebellar-specific cells. The VZ expresses pancreas transcription factor 1 subunit alpha (PTF1A), whereas the rhombic lip expresses a different basic helix-loop-helix (bHLH) transcription factor atonal homolog 1 (ATOH1/MATH1).[16]

Transcription factors play an important role in neural progenitor cell differentiation, specification, and maturation.[17–19] PTF1A is a bHLH transcription factor that is essential for neuron specification and development.[20] Its mutation leads to the failure of developing cerebellum in mouse and human.[21] The $PTF1A^+$ progenitor cells give rise to GABAergic neurons including cerebellar cortex cells (Purkinje cells and interneurons) and deep cerebellar nuclei (DCN) cells, whereas the $MATH1^+$ progenitor cells give rise to glutamatergic neurons including granule cells, brush cells, and large DCN cells.[20,22–25] The complicated structure and cell organization within the cerebellum create a challenge for cerebellar differentiation from hiPSCs. Different approaches have been investigated to recapitulate cerebellar differentiation in hiPSC-derived aggregates.[4,26,27] Most of them, however, are not efficient due to the costly factors and long-term culture that yield a low number of cells with desired markers.[28]

The most successful cerebellum differentiation method has been reported to generate the progenitors of Purkinje cells and granule cells.[4] However, progenitor maturation requires dissociation of the spheroids to select cells with desired markers before coculturing with primary mouse granule cells.[4] Retinoic acid (RA), FGFs, and Wnt signaling can affect the A-P patterning, whereas bone morphogenetic proteins (BMPs), sonic hedgehog (SHH), and Wnt can regulate the D-V patterning.[11] This study tested the hypothesis that the combination of different signaling factors, including RA, Wnt activator, and SHH activator, promotes caudal cerebellar differentiation from hiPSCs.[16,29–32] Our results demonstrate the expression of cerebellar layer markers and the characteristics of Purkinje cells based on electrophysiology. The effect of FGF8 on cerebellar development and the use of human mesenchymal stem cell-conditioned medium (hMSC-CM) after early-stage differentiation were also investigated.

Materials and Methods

hiPSC culture

Human iPSK3 cells were derived from human foreskin fibroblasts transfected with plasmid DNA encoding reprogramming factors OCT4, NANOG, SOX2, and LIN28 (kindly provided by Dr. Stephen Duncan, Medical College of Wisconsin).[33,34] Human iPSK3 cells were maintained in mTeSR Plus serum-free medium (StemCell Technologies, Inc., Vancouver, Canada) on growth factor-reduced Geltrex-coated surface (Life Technologies).[35] The cells were passaged by Accutase every 7 days and seeded at 1×10^6 cells per well of six-well plate in the presence of rho-associated protein kinase (ROCK) inhibitor Y27632 (10 μM; Sigma) for the first 24 h.[35–37]

Human Episomal iPSC (EpiPSC) cells were obtained commercially from ThermoFisher (Cat #A18945). The Gibco Human EpiPSC Line was derived from $CD34^+$ cord blood using a three-plasmid seven-factor (SOKMNLT: SOX2, OCT4, Kruppel-like factor 4-KLF4, MYC, NANOG, LIN28, and Simian vacuolating virus 40 tag-SV40L T antigen) EBNA-based episomal system. This iPSC line has zero footprint as there is no integration into the genome from the reprogramming event and is free of all reprogramming genes. Human EpiPSC cells were maintained in StemFlex™ medium (ThermoFisher) on growth factor-reduced *Matrigel*-coated surface. The cells were passaged by Versene (an EDTA-based solution; ThermoFisher) every 3–4 days and seeded at 1:8–1:12 ratio in the presence of Y27632 (10 μM) for the first 24 h. This research project used de-identified and publicly available human cell lines and does not constitute ''human subjects research'' as defined by DHHS and/or FDA regulations.

hMSC culture

Bone marrow-derived hMSCs were obtained from Tulane University. The cells were seeded at 60 cells/cm^2 and cultured in alpha modified Eagle medium (αMEM; Sigma) supplemented by 20% fetal bovine serum (FBS) (Atlanta Biologicals). The hMSC-CM was collected every 2 days and supplemented with 2% B-27 for neural culture.

Cerebellar spheroid and organoid formation from hiPSCs

In brief, human iPSK3 cells were seeded into ultra-low attachment 24-well plates (Corning Incorporated, Corning, NY) at 3×10^5 cells per well in differentiation medium composed of Dulbecco's modified Eagle's medium/nutrient mixture F-12 (DMEM/F-12) with 2% B-27 serum-free supplements (Life Technologies). Y27632 (10 μM) and TGF-β1 inhibitor SB431542 (10 μM; StemCell Technologies, Inc.) were added for the first week of culture. On day 2, FGF2 (50 ng/mL; StemCell Technologies, Inc.) was added until day 7. During the third week, FGF19 (100 ng/mL; Peprotech) was added to promote the caudalization of neural rosettes in the aggregates. Sequentially, stromal cell-derived factor 1-α (SDF1A, 50 ng/mL; Peprotech) was used in the fifth week of culture to induce the formation of the molecular layer, the Purkinje cell layer, and the granule cell layer. This procedure was used as a control condition.[4]

For experimental conditions, RA (1.0 μM; Sigma), Wnt activator CHIR99021 (CHIR, 10 μM; Sigma), or the combination of both was added to the culture at the second week (Supplementary Fig. S1). FGF8 has been suggested as a rostral patterning morphogen for cerebral cortex.[38] The influence of FGF8 (50 ng/mL; Peprotech) was evaluated during weeks 2–3. Also, purmorphamine (PMR, 2 μM; Sigma) (Supplementary Fig. S1) was added at week 5 to activate the SHH pathway and promote ventralization of the spheroids. On day 35, the gene and protein expression for cerebellar

layer markers (Supplementary Fig. S2) were characterized. A total of nine differentiation conditions were evaluated (Supplementary Table S1). The derived 3D structures <35 days were referred as ''spheroids'' and those >35 days were referred as ''organoids.''

Immunocytochemistry

The cerebellar spheroids on day 35 were replated, fixed with 4% paraformaldehyde (PFA), and permeabilized with 0.5% Triton X-100. The samples were then blocked with 2% FBS in phosphate-buffered saline (PBS) for 30 min and incubated with various mouse or rabbit primary antibodies (Supplementary Table S2) overnight at 4°C. After washing with PBS, the cells were incubated with the corresponding secondary antibody: Alexa Fluor® 488 goat antimouse IgG_1, IgG_{2b}, or Alexa Fluor 594 goat antirabbit IgG (Life Technologies) for 1 h. The samples were counterstained with Hoechst 33342 and visualized using a fluorescent microscope (Olympus IX70, Melville, NY) or a confocal microscope (Zeiss LSM 880).

Flow cytometry

To quantify various neural markers, the cells were harvested by trypsinization and analyzed by flow cytometry. In brief, 1×10^6 cells per sample were fixed with 4% PFA and washed with PBS. The cells were permeabilized with 100% cold methanol, blocked with blocking buffer, and then incubated with various primary antibodies (Supplementary Table S2) followed by the corresponding secondary antibody Alexa Fluor 488 goat antimouse IgG_1 or Alexa Fluor 594 goat antirabbit or donkey antigoat IgG. The cells were acquired with BD FACSCanto™ II flow cytometer (Becton Dickinson) and analyzed against isotype controls using FlowJo software.

Quantitative reverse transcription-polymerase chain reaction analysis

Total RNA was isolated using the RNeasy Mini Kit (Qiagen, Valencia, CA) according to the manufacturer's protocol followed by the treatment of DNA-Free RNA Kit (Zymo, Irvine, CA). Reverse transcription was carried out using 2 μg of total RNA, anchored oligo-dT primers (Operon, Huntsville, AL), and Superscript III (Invitrogen, Carlsbad, CA) (according to the protocol of the manufacturer). Primers specific for target genes (Supplementary Table S3) were designed using the Primer-BLAST (NCBI), and the melting temperature was checked using NetPrimer analysis (PREMIER Biosoft). The gene *β-actin* was used as an endogenous control for normalization of expression levels. Real-time reverse transcription-polymerase chain reactions (RT-PCRs) were performed on an ABI7500 instrument (Applied Biosystems, Foster City, CA) using SYBR1 Green PCR Master Mix (Applied Biosystems). The amplification reactions were performed as follows: 2 min at 50°C, 10 min at 95°C, and 40 cycles of 95°C for 15 s and 55°C for 30 s, and 68°C for 30 s. Fold variation in gene expression was quantified by means of the comparative $2^{-\Delta\Delta CT}$ method based on the comparison of expression of the target gene (normalized to the endogenous control β-actin) among different conditions.

Electrophysiology

Whole-cell patch clamp recording was performed at room temperature from cultured cells bathed in extracellular solution containing (in mM) 136 NaCl, 4 KCl, 2 MgCl, 10 HEPES, and 1 EGTA (312 mOsm, pH 7.39). Glass electrodes (resistance 2–6 MΩ) were filled with intracellular solution containing 130 mM KCl, 10 mM HEPES, and 5 mM EGTA (292 mOsm, pH 7.20). Cells were visualized under phase contrast with a Nikon Eclipse Ti-U inverted microscope and attached DS-Qi1 monochrome digital camera. Recordings were made with an Axopatch 200B amplifier (Molecular Devices) and digitized with a Digidata 1440A system (Molecular Devices). Ionic currents were evoked by depolarizing voltage steps at voltage clamp configuration. A current clamp protocol was applied to generate action potentials and hyperpolarization activated (Ih) potentials. Signals were filtered at 1 kHz and sampled at 10 kHz. Data were collected and analyzed using pCLAMP 10 software (Molecular Devices).

Statistical analysis

Each experiment was carried out at least three times with more than six replicates. The representative experiments are presented, and the results are expressed as (mean ± standard deviation). To assess the statistical significance, one-way ANOVA followed by Fisher's LSD *post hoc* tests was performed. A p-value <0.05 was considered statistically significant.

Results

The effects of RA, PMR, and CHIR

The combination of SB431542 (SB) and FGF2 was used to induce neural differentiation, whereas ROCK inhibitor Y-27632 was used to promote cell survival and aggregation (Supplementary Fig. 1A). RA and Wnt activator CHIR99021 (CHIR) (Supplementary Fig. 1B) were added at week 2. Caudalizing factor FGF19 was used on week 3 for neural rosette formation. In week 5, SDF1A was added to initiate neural epithelium formation with or without the ventralizing factor PMR (Supplementary Fig. 1B). The schematic differentiation protocol is shown in Figure 1A. On day 35, the spheroids were replated on *Matrigel* and stained for various neural markers. The differentiated cells from iPSK3 cells were positive for glutamate (GLUT) and γ-aminobutyric acid (GABA), the markers of glutamatergic and GABAergic neurons, respectively. In addition, the cells expressed presynaptic marker synapsin I (SYN1) and postsynaptic marker PSD95 (Fig. 1B).

The cerebellum mainly consists of Purkinje cells and the granule cells that comprise three different layers: the molecular layer that consists of Purkinje cell progenitors ($NEPH3^+/PTF1A^+$), the Purkinje cell layer ($OLIG2^+/L7^+$), and the granule cell layers ($MATH1^+/PAX6^+/GAD65^+$).[4,15] In this study, the differentiated spheroids were found to express hindbrain marker HOXB4 and markers of the molecular layer (NEPH3 and PTF1A), the Purkinje cells (OLIG2), and the granule cells (MATH1, PAX6, and GAD65) (Fig. 1C). PTF1A is a marker of the GABAergic neural progenitors and is expressed by $OLIG2^+$ cells.[39] NEPH3 is one of the downstream targets of PTF1A.[40] PAX6

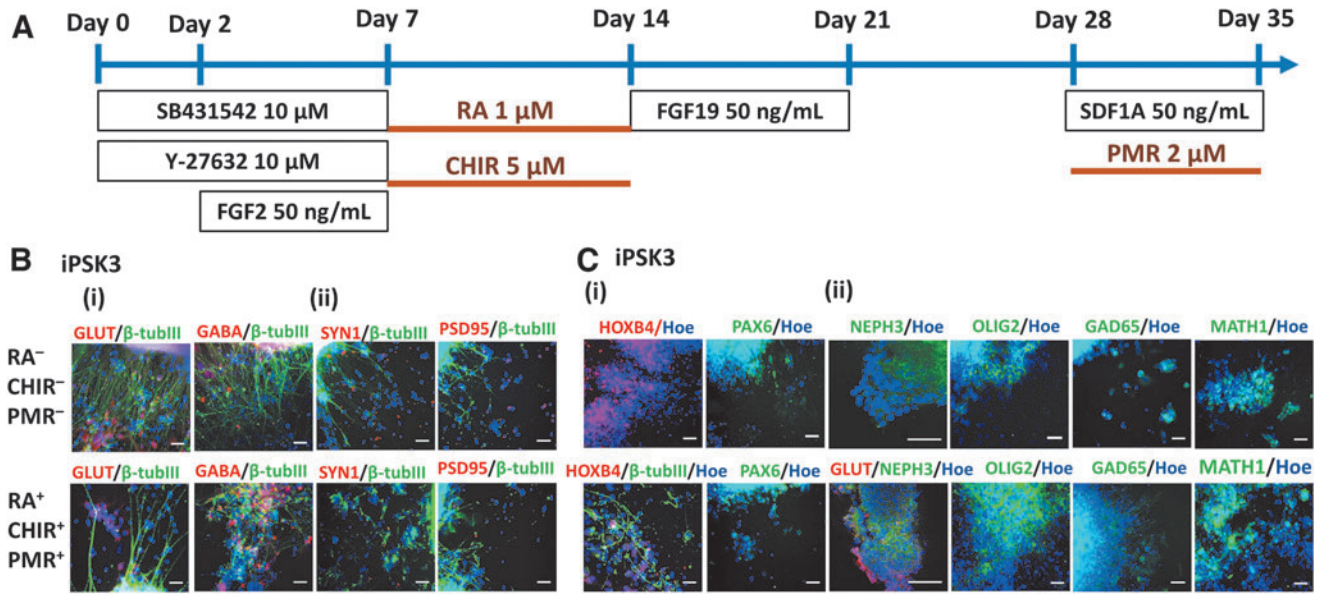

FIG. 1. The differentiation of cerebellar spheroids from iPSK3 cells. **(A)** Schematic illustration of cerebellar differentiation using iPSK3 cells. **(B)** Representative fluorescent images of day 35 replated cerebellar spheroids for common neuronal markers: **(i)** GLUT and GABA; **(ii)** SYN1 (presynaptic) and PSD95 (postsynaptic). *Blue*: Hoechst. **(C)** Representative fluorescent images of cerebellar spheroids at day 35 for neural developmental and cerebellar markers: **(i)** HOXB4 and PAX6; **(ii)** NEPH3, OLIG2, and MATH1. The NEPH3/Hoe and GLUT/NEPH3/Hoe images were taken using Zeiss LSM 880 confocal microscope, whereas the other images were taken using the Olympus IX70 fluorescent microscope. Scale bar: 100 µm.

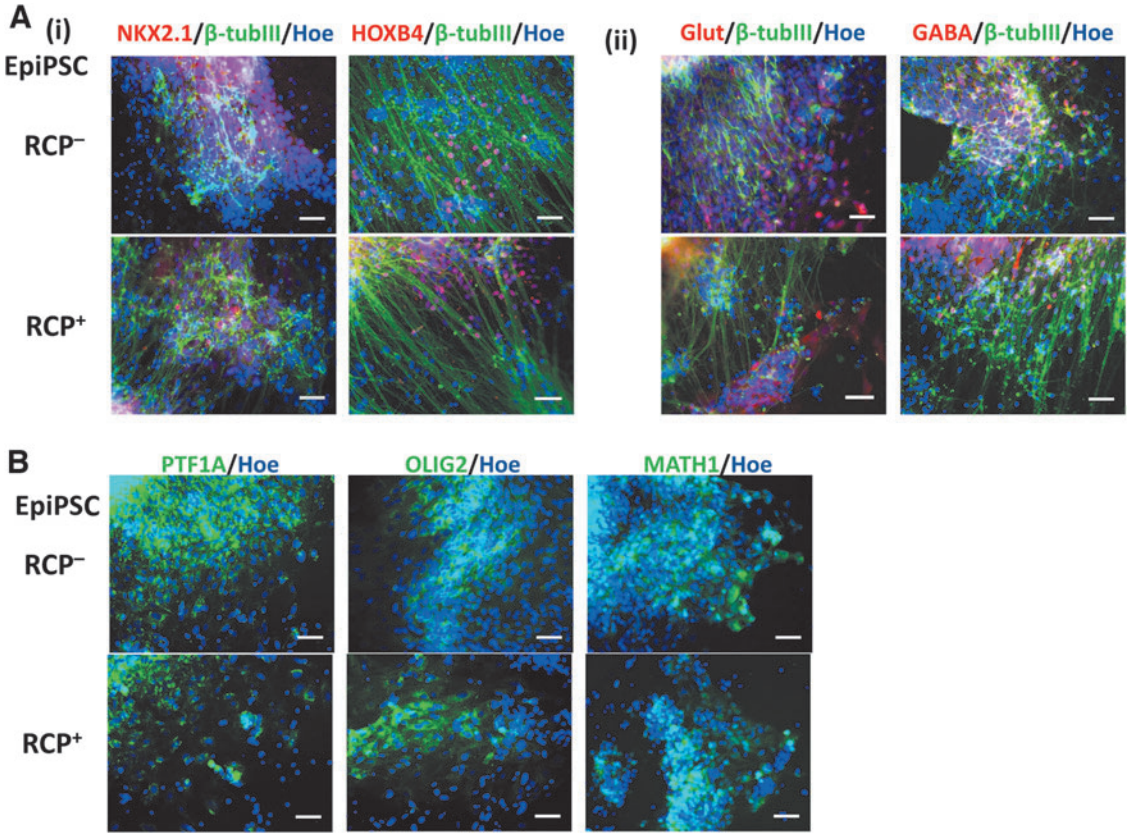

FIG. 2. Characterization of cerebellar spheroids differentiated from an episomal iPSC line (EpiPSC). With (RCP^+) or without (RCP^-) indicates the presence of RA, CHIR, and PMR. The representative fluorescent images of **(A)** common neural markers: **(i)** NKX2.1 (ventral) and HOXB4 (hindbrain) costained with β-tubulin III (β-tubIII); **(ii)** GLUT and GABA costained with β-tubulin III (β-tubIII); **(B)** the cerebellar markers PTF1A, OLIG2, and MATH1. All the images were taken using the Olympus IX70 fluorescent microscope. Scale bar: 100 µm. iPSC, induced pluripotent stem cell; PMR, purmorphamine; RA, retinoic acid.

is a marker of dorsal forebrain identity and highly expressed in the cerebral cortex's granule cells.[41,42] The induction of PAX6 promotes neuronal gene expression such as *SOX1* and *SOX2*.[16,43]

EpiPSC line was also used for cerebellar differentiation with or without the combination of RA, CHIR, and PMR (RCP). Similarly, the expression of cortical ventral marker NKX2.1/β-tubulin III, hindbrain brain marker HOXB4/β-tubulin III, Glut, and GABA was observed (Fig. 2A). The expression of cerebellar markers PTF1A, OLIG2, and MATH1 was also observed (Fig. 2B).

RT-PCR analysis showed that the RCP-untreated cerebellar spheroids had low expression of *HOXB4* and *NKX2.1*, but high expression of *TBR1*. In particular, the spheroids highly expressed cerebellar markers, including the molecular layer marker *NEPH3* (35 ± 7 vs. 0.9 ± 0.2), the Purkinje cell progenitor marker *OLIG2* (45 ± 2 vs. 0.99 ± 0.01), and the granule cell progenitor marker *MATH1* (21 ± 9 vs. 0.9 ± 0.1) (Fig. 3A). OLIG2 is a marker for Purkinje cell progenitors,[39,44] and MATH1 is a marker of early granule progenitor cell.[22,26] Therefore, the spheroids display cerebellar identity without RCP treatment.

Among the different combinations of RA (R), CHIR (C), and PMR (P), RCP-treated condition showed the most promising results. Flow cytometry showed that the RCP-treated spheroids had high expression of NEPH3 (58.8% vs. 45.2%) and PTF1A (38.0% vs. 21.3%), and general neuronal marker β-tubulin III (Fig. 3B and Supplementary Fig. S3). Also, RCP-treated spheroids had higher gene expression of *OLIG2* (1.39 ± 0.01 vs. 0.81 ± 0.01) and *MATH1* (1.90 ± 0.20 vs. 0.90 ± 0.30) compared with the untreated group, whereas the gene expression for *NEPH3* (0.16 ± 0.05 vs. 1.00 ± 0.20) is lower (Fig. 3C). In addition, the CP-treated spheroids had higher *HOXB4* expression but lower

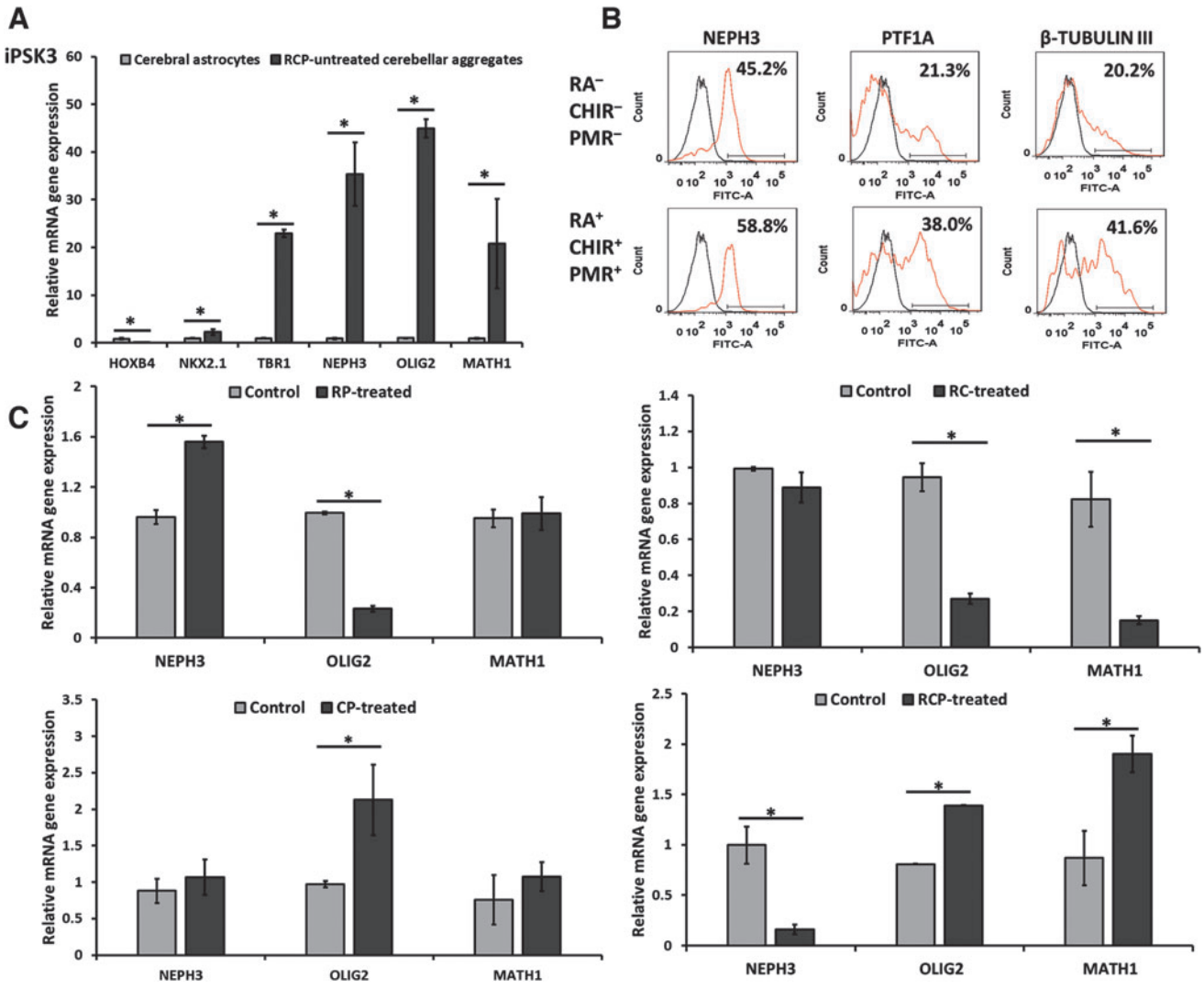

FIG. 3. Characterizations of the iPSK3-derived cerebellar spheroids at day 35. **(A)** mRNA expression of *HOXB4, NKX2.1,* and *TBR1*, and the cerebellar markers *NEPH3, OLIG2,* and *MATH1* for the cerebral astrocytes and the cerebellar spheroids ($n = 3$). *Indicates $p < 0.05$. **(B)** The replated spheroids were dissociated and characterized using flow cytometry for molecular layer markers of NEPH3 and PTF1A and general neuronal marker β-tubulin III. *Black line*: negative control, *red line*: marker of interest. **(C)** Relative mRNA expression for cerebellar markers of the derived spheroids in the presence of different combinations of retinoic acid (R), CHIR99021 (C), and purmorphamine (P) ($n = 3$). *Indicates that $p < 0.05$ between the test conditions.

TBR1 expression than the untreated control, showing a caudalization effect (Supplementary Fig. S4). Together, these results indicate that RCP treatment promotes the formation of three cerebellar layers, whereas the untreated group enriched the cells at the immature molecular layer stage.

For other combinations, both RP- and RC-treated spheroids had lower PTF1A expression (34.6% vs. 49.1% and 40.4% vs. 53.4%, respectively) (Supplementary Table S4). Gene expression analysis showed that RP-treated spheroids showed the increased *NEPH3* (1.56 ± 0.05 vs. 0.96 ± 0.06) but the decreased *OLIG2* (0.23 ± 0.02 vs. 0.99 ± 0.01) expression. CP treatment only increased *OLIG2* expression (2.1 ± 0.5 vs. 0.97 ± 0.04). RC treatment showed a decrease in *OLIG2* (0.27 ± 0.03 vs. 0.94 ± 0.08) and *MATH1* (0.823 ± 0.15 vs. 0.15 ± 0.02) (Fig. 3C).

Whole-cell patch clamp recording was performed to examine electrophysiological properties of the cells from day 80 cerebellar organoids for the RCP condition. In response to depolarizing voltages, these cells generated both fast-inactivating inward Na^+ currents and long-lasting outward K^+ currents, indicating their neuronal identity (Fig. 4A). Under the current clamp configuration, some of the cells exhibited the following voltage responses that are characteristic of cerebellar Purkinje cells: (1) injection of hyperpolarizing currents produced a depolarizing sag (Ih potential), (2) depolarizing current pulses elicited repetitive firing with waveform-like complex spikes (Fig. 4B).

Effect of FGF8

FGF8 was added for evaluating its effect on the induction of cerebellar spheroids (Fig. 5A, B). FGF8 increased the expression of the molecular layer markers NEPH3 (37.6% vs. 28.6%) and PTF1A (60.6% and 52.4%) (Fig. 5C). Confocal images also showed the formation of $PTF1A^+$ neural rosettes within the spheroids (Fig. 5D). In addition, the replated spheroids expressed the markers of ventral forebrain (NKX2.1), the hindbrain (HOXB4 and PAX6), and the deep cortical layer VI (TBR1) (Fig. 6). The expression of glutamatergic neuron markers (GLUT and VGAT), GABAergic neuron marker (GABA), and synaptic markers (SYN1 and PSD95) was also observed. FGF8-treated spheroids also showed the expression of NEPH3, OLIG2, and MATH1.

The effects of hMSC-CM on extended culture of the cerebellar organoids

After day 35, the RCP-treated spheroids were cultured in either HMSC-CM/B27 or DMEM/F12/B27 for additional 2 weeks. The replated organoids showed neural morphology on day 49. Flow cytometry analysis showed that HMSC-CM could prevent the decrease of molecular layer marker NEPH3 (47.5% vs. 28.9%), PTF1A (63.8% vs. 52.3%), and the granule cell marker MATH1 (40.2% vs. 22.2%) of the RCP-treated organoids. Gene analysis showed that

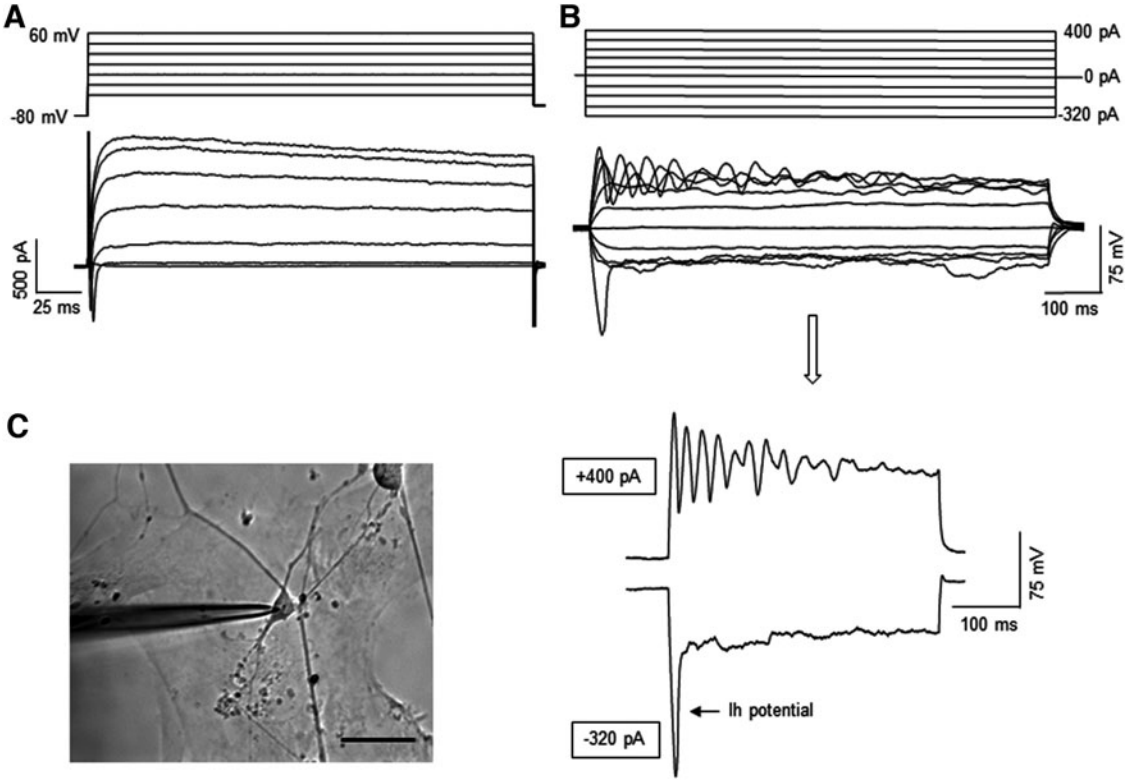

FIG. 4. Electrophysiological properties of the cells from day 80 cerebellar organoids differentiated from iPSK3 line. The day 80 cerebellar organoids were derived with RCP condition. The organoids were replated on *Matrigel*-coated coverslips and grown for 1 week before the recording. **(A)** Representative traces of voltage clamp recordings showing fast inward Na^+ currents followed by long-lasting outward K^+ currents evoked by depolarizing voltage steps. **(B)** Representative traces of current clamp recordings showing voltage responses to stepwise current injections. Repetitive action potentials were evoked by depolarizing (+400 pA) current injection, whereas Ih potential was elicited by hyperpolarizing (−320 pA) current injection. **(C)** Phase contrast image of the patch clamp recoding; scale bar: 50 μm.

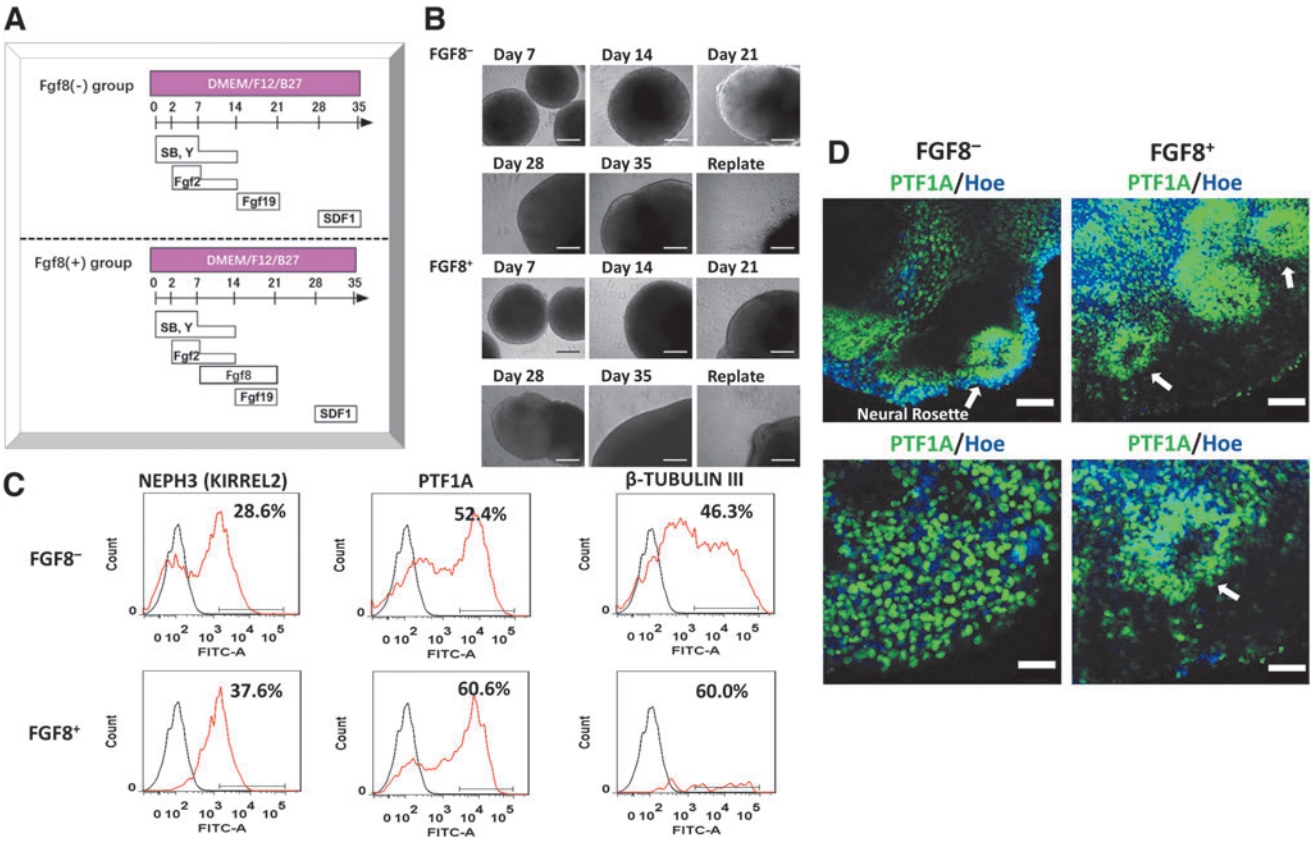

FIG. 5. The effects of FGF8 on the differentiation of cerebellar spheroids using iPSK3 cells. **(A)** FGF8 was added during weeks 2 and 3 of the differentiation. **(B)** The phase contrast images of the cerebellar spheroids for 35 days were taken using the Olympus IX70. Scale bar: 200 μm. **(C)** Representative flow cytometry histograms of cerebellar molecular layer markers NEPH3 and PTF1A. *Black line*: negative control, *red line*: marker of interest. **(D)** The confocal fluorescent images of the cerebellar spheroids for PTF1A were taken using the Zeiss LSM 880 microscope. The *white arrows* point toward the neural rosettes. Scale bar: 100 μm (*tops*) and 50 μm (*bottoms*).

HMSC-CM supported higher gene expression of *NEPH3* (0.90 ± 0.10 vs. 0.35 ± 0.02), *OLIG2* (0.80 ± 0.20 vs. 0.10 ± 0.04), and *MATH1* (0.80 ± 0.20 vs. 0.24 ± 0.07) (Fig. 7).

Discussion

This study investigated the effects of RA, CHIR, and PMR on the development of the three cerebellar layers, the effects of FGF8 on the development of molecular layer, and the effects of hMSC-CM on the maturation of cerebellar spheroids from hiPSCs (Supplementary Fig. S5–S8).

Effects of the combination of RA, CHIR, and PMR on cerebellar differentiation

FGF8, various Wnt ligands, and BMPs could induce the expression of granule cell markers with a small population of CALB1$^+$ Purkinje cells from embryoid bodies.[26] Co-culturing early stage cerebellar spheroids with mouse cerebellar cells yielded a low number of CALB$^+$ cells in long-term culture.[45] The combination of FGF8 with Wnt has been shown to induce early cerebellar differentiation, and SHH treatment produced a small number of Purkinje cells and astrocytes.[27] FGF19 can promote the caudalization and neural-tube-like epithelium structure with D-V polarity, and when combined with FGF2 and SDF1A, it promotes neural epithelium sheet that displays apicobasal polarization similar to the cerebellar layer.[4] Therefore, sequentially treating the spheroids with RA, Wnt activator, and SHH activator in addition to FGF2, FGF19, and SDF1A should promote PTF1A$^+$ Purkinje progenitors and MATH1$^+$ granule progenitors as shown in this study. PTF1A is essential for deriving all the neuronal subtypes in the VZ, including Purkinje cells.[20,46]

This study investigated the effects of caudalization factors RA, Wnt activator CHIR, and ventralization factor PMR on cerebellar differentiation of hiPSCs. Different combinations of these factors promoted the formation of different brain regions. Combining RA with SHH recapitulates the *in vivo* signaling pathway and was shown to produce spinal motor neurons.[31] Wnt inhibition has been shown to induce cerebral cortex formation and rostral marker expression[7,47]; therefore, Wnt activation favors hindbrain formation. D-V axis is governed mainly by ventralizing SHH and the antagonized Wnt and BMP pathways for dorsalization.[48–50] SHH signaling with or without the inhibition of Wnt signaling promotes ventral telencephalic cells in the cortex.[16,51,52] CHIR was shown to activate the Wnt pathway and enrich cells of forebrain (low Wnt), midbrain (medium Wnt), and hindbrain and spinal cord (high Wnt).[30] So activation of Wnt can promote the rostrocaudal axis formation in a dose-dependent

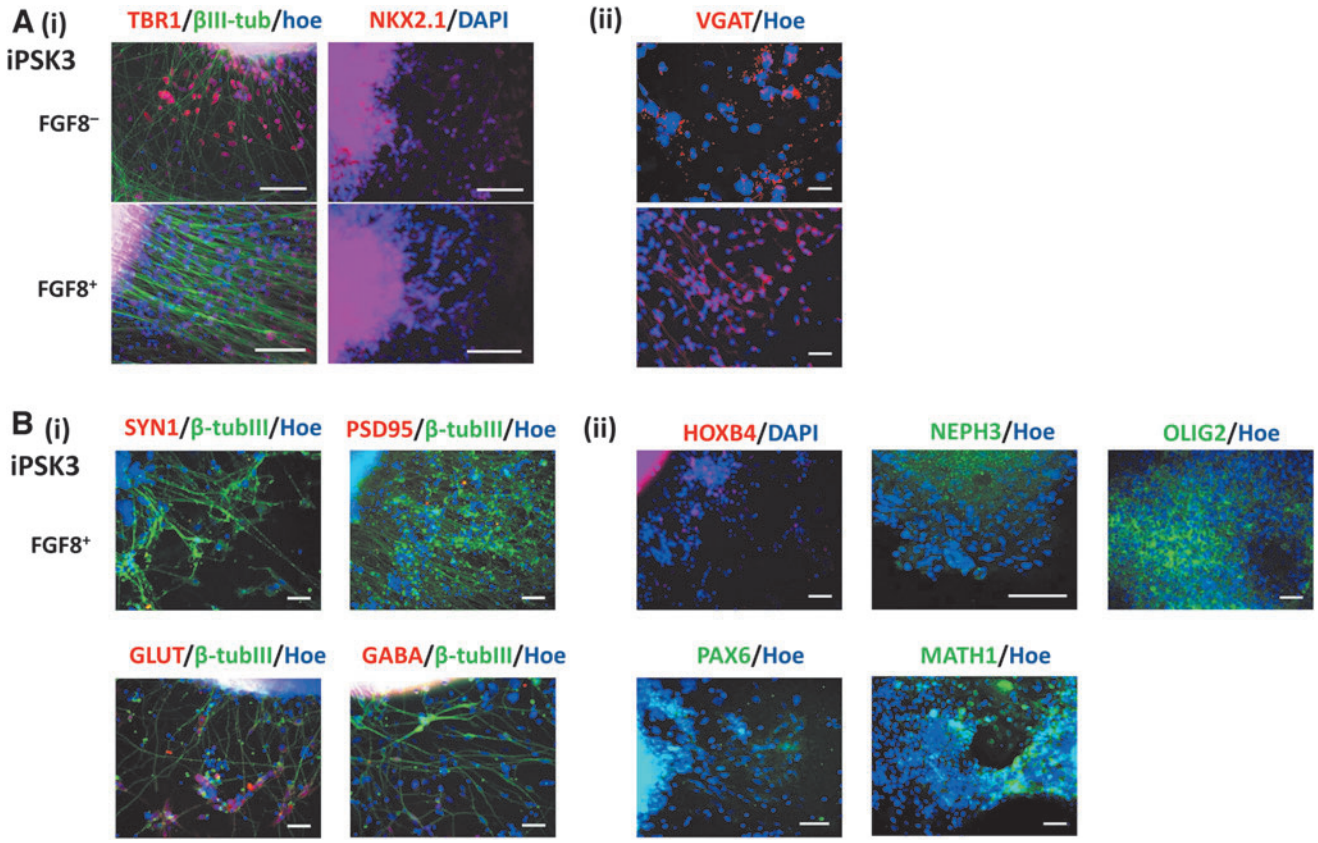

FIG. 6. Phenotypic characterization of the cerebellar spheroids cultured with or without FGF8. The fluorescent images of **(A)** the cortical layer IV marker TBR1 and the ventral neuronal marker NKX2.1, **(B)** the common neural markers of **(i)** SYN1, PSD95, GLUT, and GABA; **(ii)** the brain regional markers of **(ii)** HOXB4, PAX6, and NEPH3. The NEPH3/Hoe image was taken using Zeiss LSM 880 confocal microscope, whereas the other images were taken using the Olympus IX70 fluorescent microscope. Scale bar: 100 μm.

manner.[30] Wnt also induces the differentiation of ventral midbrain enriched with dopamineregic neurons and hindbrain serotonin neurons from hiPSCs.[9,53] Inhibition of Wnt usually promotes the differentiation of hiPSCs into forebrain cells.[5,54]

SHH activation results in the differentiation of OLIG2$^+$ motor neuron progenitors, and the combination of SHH and CHIR has been reported to generate >90% OLIG2$^+$ neurons.[55] OLIG2, an oligodendrocyte-specific bHLH, is expressed in the cerebellar neuroepithelium of the hindbrain.[56] In the mouse cerebellum, OLIG2 is expressed in the VZ during the E11.5 to E13.5 of the development, which is also the peak time of Purkinje cell development.[39] OLIG2$^+$ cells can differentiate into Purkinje cells, and the loss of OLIG2 decreases the number of Purkinje cells.[39,44]

Our study showed that the addition of caudalization factors can promote the expression of markers for Purkinje progenitors and granule progenitors on day 35. In addition, SDF1A decreases the expression of ventral markers,[4] but its effect might be improved by PMR. RA has been shown to prevent cerebellar differentiation, possibly by decreasing the midbrain–hindbrain boundary markers of FGF8 and Wnt.[4] However, RA is important not only for hindbrain patterning but also for neurite outgrowth.[57] In our study, RC treatment decreased the OLIG2$^+$ cells, and RC-treated spheroids expressed lower levels of *OLIG2* and *MATH1*. SHH activation by PMR can promote *MATH1* expression and increase the population of Purkinje cells.[26] Therefore, combining RC with PMR (RCP) should promote the expression of *OLIG2* and *MATH1*. Our gene analysis showed that RCP-treated spheroids expressed a higher level of *OLIG2* and *MATH1*. Also, RCP treatment results in 42.0% and 46.4% of OLIG2$^+$ and MATH1$^+$ cells, respectively. In contrast, when comparing RP with RCP treatment, CHIR increased the expression of Purkinje and granule cell markers. RCP treatment can increase *OLIG2* and *MATH1* expression at the expense of *NEPH3*, which might suggest the maturation of cerebellar spheroids.

The cerebellar spheroids were also positive for neural markers PAX6, TBR1, HOXB4, and NKX2.1. PAX6 is expressed in glutamatergic neuron progenitors in VZ of dorsal telencephalon.[58] PAX6 upregulates the expression of Neurogenin 2 (NGN2), which is a bHLH that induces the differentiation of glutamatergic neurons.[59–61] NGN2 then induces the expression of TBR2 and promotes the expression of neurogenic differentiation (NeuroD) and TBR1.[59,62] TBR1 is expressed in deep cortical layer VI neurons, and *TBR1*-deficienct mice lacked subplate or layer VI neurons.[63]

The *HOX* gene family plays an important role in embryonic development and lineage specification such as the hematopoietic system and hindbrain segmentation.[64–66] *HOXB4* expression in the hindbrain is induced by activation

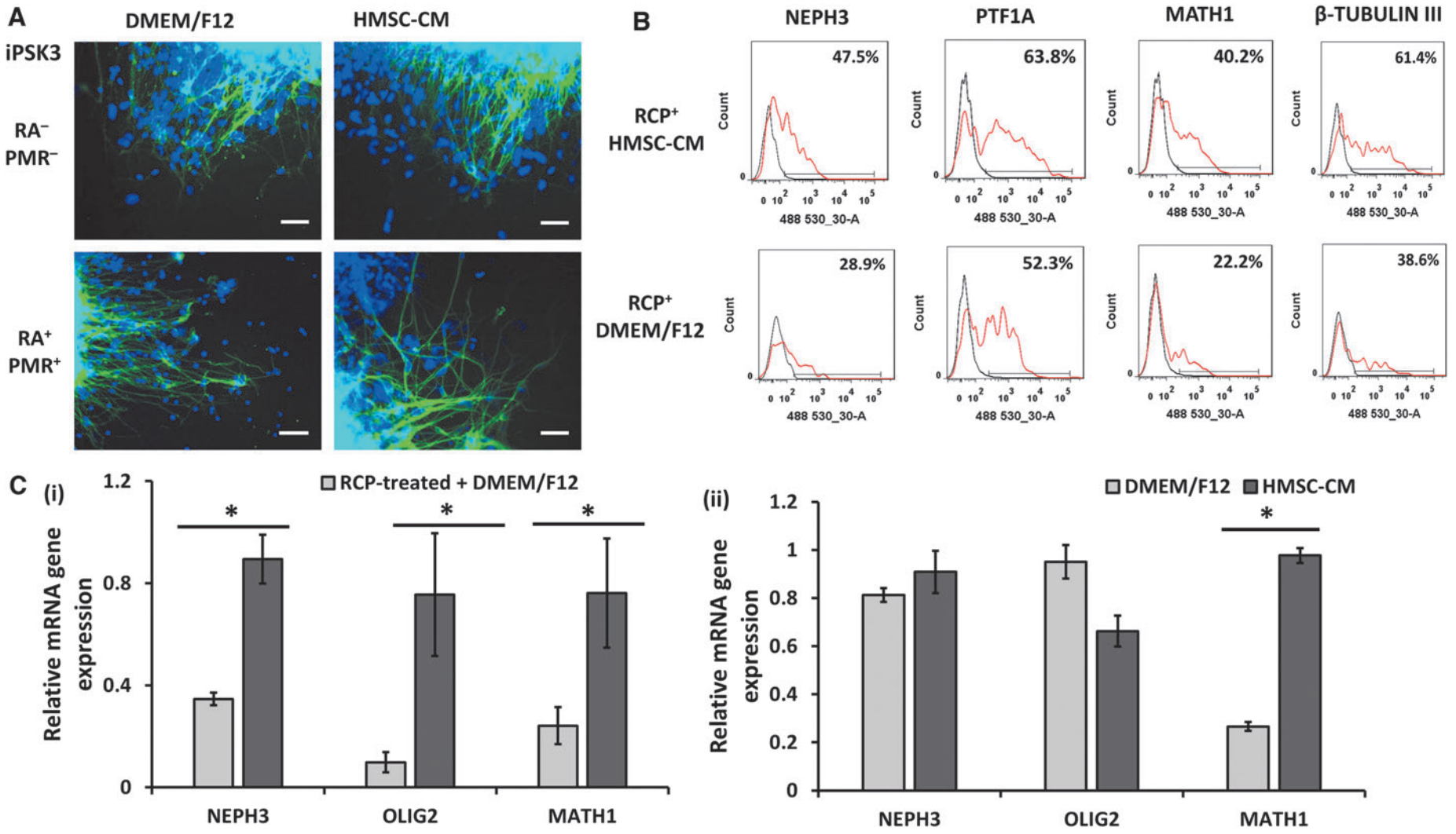

FIG. 7. The effects of hMSC-CM on the marker expression of cerebellar organoids. **(A)** The fluorescent images of RP-treated organoids on day 49 were taken using the Olympus IX70 fluorescent microscope. They were either cultured in DMEM/F12 plus B27 or hMSC-CM/FBS plus B27. Scale bar: 100 μm. **(B)** Representative flow cytometry histograms of NEPH3, PTF1A, and β-tubulin III for cells in different cultured media. *Black line*: negative control, *red line*: marker of interest. **(C)** mRNA expression of cerebellar layer markers of *NEPH3, OLIG2,* and *MATH1* of the **(i)** RCP-treated and the **(ii)** untreated organoids cultured in HMSC-CM or DMEM/F12 condition ($n=3$). *Indicates $p<0.05$. hMSC-CM, human mesenchymal stem cell-conditioned medium.

of the retinoid pathway through activation of RA receptors.[67] The *NKX2.1*-deficient mice had a lower number of $GABA^+$ and $CALB^+$ cells, that is, Purkinje cells.[68] In addition, mouse embryos with *NKX2.1* mutation showed lower SHH expression level, which can cause the histological defects along the D-V axis.[50,68]

The Purkinje cells enrich the GABAergic neurons derived from the VZ.[69] Our electrophysiology results of RCP condition demonstrated fast-inactivating inward Na^+ and long-lasting outward K^+ currents. Some of the cells also showed a depolarizing sac when subjected to hyperpolarizing current and depolarizing current pulses with repetitive firing with waveform-like peaks, which are the characteristics of Purkinje cells. These electrophysiological results confirm the presence of Purkinje cells within cerebellar organoids in our study.

Effects of FGF8 on cerebellar differentiation

After the isthmic organization formation, Wnt and FGF8 are produced in a feedback loop to regulate the midbrain and hindbrain regions through the expression of Otx2 (a forebrain and midbrain marker) and GBX2 (a hindbrain marker).[13] FGF8, however, is a rostrocaudal patterning molecule and regulates the transcription factors involved in the specification of different brain regions.[70,71] The role of FGF8 in the mouse brain is inconclusive because FGF8 was reported to promote hindbrain and cerebellum differentiation as well as the identity of cerebral cortex in mice.[26,72] FGF8 also has little effect on patterning the neural epithelium into midbrain–hindbrain fate.[73,74]

Our flow cytometry results showed the expression of the molecular layer markers with or without FGF8 treatment. The spheroids were found to contain both GABAergic and glutamatergic neurons. In another study, neural induction of hiPSCs exhibited rostral areas but not the middle and caudal regions,[38] meaning that the presence of FGF8 might not be needed for cerebellar development and differentiation.

The effects of hMSC-CM in long-term culture of the cerebellar spheroids

Various attempts have been made to mature the cerebellar progenitors into Purkinje cells and granule cells. For instance, the treatment with human brain-derived neurotrophic factor and neurotrophin 3 induced the maturation of cerebellar spheroids during a long-term culture, resulting in 11.9% of $CALB^+$ cells (i.e., Purkinje cells).[45] In a different study, various BMPs combined with SHH and neurotrophic factors generated 11% of $PCP2^+$ cells (also Purkinje cells).[27] To improve cerebellar maturation, hMSC-CM was investigated for prolonged differentiation in this study.

Ataxia is the degeneration of neuron connection, and spinocerebellar ataxia (SCA) mainly affects the Purkinje cells dendrite and atrophy.[75] MSC transplantation can improve the function of Purkinje cells by increasing dendrites formation, thickening the molecular deep layer, decreasing apoptotic cells, and producing extracellular matrices (ECMs) and neural trophic factors.[75] In SCA mice, MSC treatment was reported to improve rotatory without tumor formation.[76] MSCs can migrate to the Purkinje cell regions and secrete neurotrophic factors as well as MMP2 and MMP3 to improve neural development.[77,78] Clinical trials and the case study of injecting MSCs into cerebellum have been evaluated for the safety and efficacy.[79,80] Therefore, hMSC-CM might be able to improve the maturation of hiPSC-derived cerebellar spheroids.

In our study, hMSC-CM was found to promote the markers for the molecular layer, the Purkinje cell layer, and the granule cell layer for the RCP-treated spheroids. The positive effects of hMSC-CM may be attributed to the release of the growth factors and cytokines, including hepatocyte growth factor, FGF2, IGF1, and VEGF.[81] IGF and VEGF were reported to increase neurogenesis at both protein and gene expression levels.[82] The secreted ECMs can also promote neural cell growth.[83] In addition, MSCs were reported to release neurotrophic factors, reduce inflammation and free radicals, inhibit apoptosis, and promote differentiation of neural stem cells.[84]

Conclusions

In summary, the cerebellar organoids were derived from two hiPSC lines, which expressed cerebellar markers of the three layers. In addition, the combination of RA, CHIR, and PMR can further promote the gene expression of Purkinje cell layer and the granule cell layer. The cerebellar organoids contain cells expressing Purkinje cell electrophysiology and biomarkers. Our approach yields a high percentage of Purkinje cells and granule cells and does not require the use of mouse feeder layer. This study should advance the understanding of different morphogens on cerebellar development of the human brain.

Acknowledgments

The authors thank Ms. Ruth Didier from the Flow Cytometry Laboratory of FSU Department of Biomedical Sciences for her assistance, Dr. Brian K. Washburn and Kristina Poduch from the Molecular Cloning Facility of FSU Department of Biological Sciences for their help with qRT-PCR analysis, Dr. Stephen Duncan of Medical College of Wisconsin and Dr. David Gilbert of FSU Department of Biological Sciences for human iPSK3 cells.

Disclosure Statement

No competing financial interests exist.

Funding Information

This study was supported by NSF Career Award (Grant No. 1652992 to Y.L.) and Florida Department of Health (FDOH) Live Like Bella Award (Grant No. 9LA01 to Q.X.A.S. and Y.L.).

Supplementary Material

Supplementary Figure S1
Supplementary Figure S2
Supplementary Figure S3
Supplementary Figure S4
Supplementary Figure S5
Supplementary Figure S6
Supplementary Figure S7
Supplementary Figure S8

Supplementary Table S1
Supplementary Table S2
Supplementary Table S3
Supplementary Table S4

References

1. Thomson, J.A., Itskovitz-Eldor, J., Shapiro, S.S., Waknitz, M.A., Swiergiel, J.J., Marshall, V.S., *et al.* Embryonic stem cell lines derived from human blastocysts. Science **282,** 1145, 1998.
2. Passier, R., Orlova, V., and Mummery, C. Complex tissue and disease modeling using hiPSCs. Cell Stem Cell **18,** 309, 2016.
3. Di Lullo, E., and Kriegstein, A.R. The use of brain organoids to investigate neural development and disease. Nat Rev Neurosci **18,** 573, 2017.
4. Muguruma, K., Nishiyama, A., Kawakami, H., Hashimoto, K., and Sasai, Y. Self-organization of polarized cerebellar tissue in 3D culture of human pluripotent stem cells. Cell Rep **10,** 537, 2015.
5. Kadoshima, T., Sakaguchi, H., Nakano, T., Soen, M., Ando, S., Eiraku, M., *et al.* Self-organization of axial polarity, inside-out layer pattern, and species-specific progenitor dynamics in human ES cell-derived neocortex. Proc Natl Acad Sci U S A **110,** 20284, 2013.
6. Maroof, A.M., Keros, S., Tyson, J.A., Ying, S.-W., Ganat, Y.M., Merkle, F.T., *et al.* Directed differentiation and functional maturation of cortical interneurons from human embryonic stem cells. Cell Stem Cell **12,** 559, 2013.
7. Imaizumi, K., Sone, T., Ibata, K., Fujimori, K., Yuzaki, M., Akamatsu, W., *et al.* Controlling the regional identity of hPSC-derived neurons to uncover neuronal subtype specificity of neurological disease phenotypes. Stem Cell Rep **5,** 1010, 2015.
8. Lippmann, E.S., Williams, C.E., Ruhl, D.A., Estevez-Silva, M.C., Chapman, E.R., Coon, J.J., *et al.* Deterministic HOX patterning in human pluripotent stem cell-derived neuroectoderm. Stem Cell Rep **4,** 632, 2015.
9. Lu, J., Zhong, X., Liu, H., Hao, L., Huang, C.T.-L., Sherafat, M.A., *et al.* Generation of serotonin neurons from human pluripotent stem cells. Nat Biotechnol **34,** 89, 2016.
10. Roostaei, T., Nazeri, A., Sahraian, M.A., and Minagar, A. The human cerebellum: a review of physiologic neuroanatomy. Neurol Clin **32,** 859, 2014.
11. Tao, Y., and Zhang, S.-C. Neural subtype specification from human pluripotent stem cells. Cell Stem Cell **19,** 573, 2016.
12. Canning, C.A., Lee, L., Irving, C., Mason, I., and Jones, C.M. Sustained interactive Wnt and FGF signaling is required to maintain isthmic identity. Dev Biol **305,** 276, 2007.
13. Joyner, A.L., Liu, A., and Millet, S. Otx2, Gbx2 and Fgf8 interact to position and maintain a mid-hindbrain organizer. Curr Opin Cell Biol **12,** 736, 2000.
14. Wurst, W., and Bally-Cuif, L. Neural plate patterning: upstream and downstream of the isthmic organizer. Nat Rev Neurosci **2,** 99, 2001.
15. Martinez, S., Andreu, A., Mecklenburg, N., and Echevarria, D. Cellular and molecular basis of cerebellar development. Front Neuroanat **7,** 1, 2013.
16. Suzuki, I.K., and Vanderhaeghen, P. Is this a brain which I see before me? Modeling human neural development with pluripotent stem cells. Development **142,** 3138, 2015.
17. Kavyanifar, A., Turan, S., and Lie, D.C. SoxC transcription factors: multifunctional regulators of neurodevelopment. Cell Tissue Res **371,** 91, 2018.
18. Wang, J.W., and Stifani, S. Roles of Runx genes in nervous system development. Adv Exp Med Biol **962,** 103, 2017.
19. Cave, C., and Sockanathan, S. Transcription factor mechanisms guiding motor neuron differentiation and diversification. Curr Opin Neurobiol **53,** 1, 2018.
20. Hoshino, M., Nakamura, S., Mori, K., Kawauchi, T., Terao, M., Nishimura, Y. V., *et al.* Ptf1a, a bHLH transcriptional gene, defines GABAergic neuronal fates in cerebellum. Neuron **47,** 201, 2005.
21. Sellick, G.S., Barker, K.T., Stolte-Dijkstra, I., Fleischmann, C., Coleman, R.J., Garrett, C., *et al.* Mutations in PTF1A cause pancreatic and cerebellar agenesis. Nat Genet **36,** 1301, 2004.
22. Ben-Arie, N., Bellen, H.J., Armstrong, D.L., McCall, A.E., Gordadze, P.R., Guo, Q., *et al.* Math1 is essential for genesis of cerebellar granule neurons. Nature **390,** 169, 1997.
23. Machold, R., and Fishell, G. Math1 is expressed in temporally discrete pools of cerebellar rhombic-lip neural progenitors. Neuron **48,** 17, 2005.
24. Wang, V.Y., Rose, M.F., and Zoghbi, H.Y. Math1 expression redefines the rhombic lip derivatives and reveals novel lineages within the brainstem and cerebellum. Neuron **48,** 31, 2005.
25. Fink, A.J., Englund, C., Daza, R.A.M., Pham, D., Lau, C., Nivison, M., *et al.* Development of the deep cerebellar nuclei: transcription factors and cell migration from the rhombic lip. J Neurosci **26,** 3066, 2006.
26. Salero, E., and Hatten, M.E. Differentiation of ES cells into cerebellar neurons. Proc Natl Acad Sci U S A **104,** 2997, 2007.
27. Erceg, S., Ronaghi, M., Zipancic, I., Lainez, S., Roselló, M.G., Xiong, C., *et al.* Efficient differentiation of human embryonic stem cells into functional cerebellar-like cells. Stem Cells Dev **19,** 1745, 2010.
28. Watson, L.M., Wong, M.M.K., and Becker, E.B.E. Induced pluripotent stem cell technology for modelling and therapy of cerebellar ataxia. Open Biol **5,** 150056, 2015.
29. Elkabetz, Y., Panagiotakos, G., Al Shamy, G., Socci, N.D., Tabar, V., and Studer, L. Human ES cell-derived neural rosettes reveal a functionally distinct early neural stem cell stage. Genes Dev **22,** 152, 2008.
30. Kirkeby, A., Grealish, S., Wolf, D.A., Nelander, J., Wood, J., Lundblad, M., *et al.* Generation of regionally specified neural progenitors and functional neurons from human embryonic stem cells under defined conditions. Cell Rep **1,** 703, 2012.
31. Wichterle, H., Lieberam, I., Porter, J.A., and Jessell, T.M. Directed differentiation of embryonic stem cells into motor neurons. Cell **110,** 385, 2002.
32. Zeng, H., Guo, M., Martins-Taylor, K., Wang, X., Zhang, Z., Park, J.W., *et al.* Specification of region-specific neurons including forebrain glutamatergic neurons from human induced pluripotent stem cells. PLoS One **5,** e11853, 2010.
33. Si-Tayeb, K., Noto, F.K., Sepac, A., Sedlic, F., Bosnjak, Z.J., Lough, J.W., *et al.* Generation of human induced pluripotent stem cells by simple transient transfection of plasmid DNA encoding reprogramming factors. BMC Dev Biol **10,** 81, 2010.
34. Si-Tayeb, K., Noto, F.K., Nagaoka, M., Li, J., Battle, M.A., Duris, C., *et al.* Highly efficient generation of human

hepatocyte-like cells from induced pluripotent stem cells. Hepatology **51,** 297, 2010.
35. Yan, Y., Martin, L.M., Bosco, D.B., Bundy, J.L., Nowakowski, R.S., Sang, Q.-X.A.X.A., *et al.* Differential effects of acellular embryonic matrices on pluripotent stem cell expansion and neural differentiation. Biomaterials **73,** 231, 2015.
36. Bejoy, J., Song, L., Zhou, Y., and Li, Y. Wnt/Yes-associated protein interactions during neural tissue patterning of human induced pluripotent stem cells. Tissue Eng Part A **24,** 546, 2018.
37. Song, L., Wang, K., Li, Y., and Yang, Y. Nanotopography promoted neuronal differentiation of human induced pluripotent stem cells. Colloids Surf B Biointerfaces **148,** 49, 2016.
38. Imaizumi, K., Fujimori, K., Ishii, S., Otomo, A., Hosoi, Y., Miyajima, H., *et al.* Rostrocaudal areal patterning of human psc-derived cortical neurons by FGF8 signaling. eNeuro **5,** 1, 2018.
39. Seto, Y., Ishiwata, S., and Hoshino, M. Characterization of Olig2 expression during cerebellar development. Gene Expr Patterns **15,** 1, 2014.
40. Nishida, K., Hoshino, M., Kawaguchi, Y., and Murakami, F. Ptf1a directly controls expression of immunoglobulin superfamily molecules Nephrin and Neph3 in the developing central nervous system. J Biol Chem **285,** 373, 2010.
41. Stoykova, A., and Gruss, P. Roles of Pax-genes in developing and adult brain as suggested by expression patterns. J Neurosci **14,** 1395, 1994.
42. Stoykova, A., Fritsch, R., Walther, C., and Gruss, P. Forebrain patterning defects in Small eye mutant mice. Development **122,** 3453, 1996.
43. Zhang, X., Huang, C.T., Chen, J., Pankratz, M.T., Xi, J., Li, J., *et al.* Pax6 is a human neuroectoderm cell fate determinant. Cell Stem Cell **7,** 90, 2010.
44. Seto, Y., Nakatani, T., Masuyama, N., Taya, S., Kumai, M., Minaki, Y., *et al.* Temporal identity transition from Purkinje cell progenitors to GABAergic interneuron progenitors in the cerebellum. Nat Commun **5,** 3337, 2014.
45. Watson, L.M., Wong, M.M.K., Vowles, J., Cowley, S.A., and Becker, E.B.E. A Simplified method for generating purkinje cells from human-induced pluripotent stem cells. Cerebellum **17,** 419, 2018.
46. Pascual, M., Abasolo, I., Mingorance-Le Meur, A., Martínez, A., Del Rio, J.A., Wright, C.V.E., *et al.* Cerebellar GABAergic progenitors adopt an external granule cell-like phenotype in the absence of Ptf1a transcription factor expression. Proc Natl Acad Sci U S A **104,** 5193, 2007.
47. Motono, M., Ioroi, Y., Ogura, T., and Takahashi, J. WNT-C59, a small-molecule WNT inhibitor, efficiently induces anterior cortex that includes cortical motor neurons from human pluripotent stem cells. Stem Cells Transl Med **5**, 552, 2016.
48. Kiecker, C., and Lumsden, A. The role of organizers in patterning the nervous system. Annu Rev Neurosci **35,** 347, 2012.
49. Le Dréau, G., and Martí, E. Dorsal-ventral patterning of the neural tube: a tale of three signals. Dev Neurobiol **72,** 1471, 2012.
50. Ribes, V., and Briscoe, J. Establishing and interpreting graded Sonic Hedgehog signaling during vertebrate neural tube patterning: the role of negative feedback. Cold Spring Harb Perspect Biol **1,** a002014, 2009.
51. Danjo, T., Eiraku, M., Muguruma, K., Watanabe, K., Kawada, M., Yanagawa, Y., *et al.* Subregional specification of embryonic stem cell-derived ventral telencephalic tissues by timed and combinatory treatment with extrinsic signals. J Neurosci **31,** 1919, 2011.
52. Li, X.-J., Zhang, X., Johnson, M.A., Wang, Z.-B., Lavaute, T., and Zhang, S.-C. Coordination of sonic hedgehog and Wnt signaling determines ventral and dorsal telencephalic neuron types from human embryonic stem cells. Development **136,** 4055, 2009.
53. Kee, N., Volakakis, N., Kirkeby, A., Dahl, L., Storvall, H., Nolbrant, S., *et al.* Single-cell analysis reveals a close relationship between differentiating dopamine and subthalamic nucleus neuronal lineages. Cell Stem Cell **20,** 29, 2017.
54. Watanabe, K., Kamiya, D., Nishiyama, A., Katayama, T., Nozaki, S., Kawasaki, H., *et al.* Directed differentiation of telencephalic precursors from embryonic stem cells. Nat Neurosci **8,** 288, 2005.
55. Du, Z.-W., Chen, H., Liu, H., Lu, J., Qian, K., Huang, C.-L., *et al.* Generation and expansion of highly pure motor neuron progenitors from human pluripotent stem cells. Nat Commun **6,** 6626, 2015.
56. Takebayashi, H., Ohtsuki, T., Uchida, T., Kawamoto, S., Okubo, K., Ikenaka, K., *et al.* Non-overlapping expression of Olig3 and Olig2 in the embryonic neural tube. Mech Dev **113,** 169, 2002.
57. Maden, M., Gale, E., Kostetskii, I., and Zile, M. Vitamin A-deficient quail embryos have half a hindbrain and other neural defects. Curr Biol **6,** 417, 1996.
58. Kroll, T.T., and O'Leary, D.D.M. Ventralized dorsal telencephalic progenitors in Pax6 mutant mice generate GABA interneurons of a lateral ganglionic eminence fate. Proc Natl Acad Sci U S A **102,** 7374, 2005.
59. Osumi, N., Shinohara, H., Numayama-Tsuruta, K., and Maekawa, M. Concise review: Pax6 transcription factor contributes to both embryonic and adult neurogenesis as a multifunctional regulator. Stem Cells **26,** 1663, 2008.
60. Scardigli, R., Bäumer, N., Gruss, P., Guillemot, F., and Le Roux, I. Direct and concentration-dependent regulation of the proneural gene Neurogenin2 by Pax6. Development **130,** 3269, 2003.
61. Bertrand, N., Castro, D.S., and Guillemot, F. Proneural genes and the specification of neural cell types. Nat Rev Neurosci **3,** 517, 2002.
62. Hevner, R.F., Hodge, R.D., Daza, R.A.M., and Englund, C. Transcription factors in glutamatergic neurogenesis: conserved programs in neocortex, cerebellum, and adult hippocampus. Neurosci Res **55,** 223, 2006.
63. Hevner, R.F., Shi, L., Justice, N., Hsueh, Y., Sheng, M., Smiga, S., *et al.* Tbr1 regulates differentiation of the preplate and layer 6. Neuron **29,** 353, 2001.
64. Sauvageau, G., Thorsteinsdottir, U., Eaves, C.J., Lawrence, H.J., Largman, C., Lansdorp, P.M., *et al.* Overexpression of HOXB4 in hematopoietic cells causes the selective expansion of more primitive populations in vitro and in vivo. Genes Dev **9,** 1753, 1995.
65. Gavalas, A., Davenne, M., Lumsden, A., Chambon, P., and Rijli, F.M. Role of Hoxa-2 in axon pathfinding and rostral hindbrain patterning. Development **124,** 3693, 1997.
66. Gavalas, A., Studer, M., Lumsden, A., Rijli, F.M., Krumlauf, R., and Chambon, P. Hoxa1 and Hoxb1 synergize in patterning the hindbrain, cranial nerves and second pharyngeal arch. Development **125,** 1123, 1998.

67. Gould, A., Itasaki, N., and Krumlauf, R. Initiation of rhombomeric Hoxb4 expression requires induction by somites and a retinoid pathway. Neuron **21,** 39, 1998.
68. Sussel, L., Marin, O., Kimura, S., and Rubenstein, J.L.R. Loss of Nkx2.1 homeobox gene function results in a ventral to dorsal molecular respecification within the basal telencephalon: evidence for a transformation of the pallidum into the striatum. Development **126,** 3359, 1999.
69. Lu, Q.R., Yuk, D., Alberta, J.A., Zhu, Z., Pawlitzky, I., Chan, J., *et al.* Sonic hedgehog—regulated oligodendrocyte lineage genes encoding bHLH proteins in the mammalian central nervous system. Neuron **25,** 317, 2000.
70. Toyoda, R., Assimacopoulos, S., Wilcoxon, J., Taylor, A., Feldman, P., Suzuki-Hirano, A., *et al.* FGF8 acts as a classic diffusible morphogen to pattern the neocortex. Development **137,** 3439, 2010.
71. Fukuchi-Shimogori, T., and Grove, E.A. Emx2 patterns the neocortex by regulating FGF positional signaling. Nat Neurosci **6,** 825, 2003.
72. Fukuchi-Shimogori, T., and Grove, E.A. Neocortex patterning by the secreted signaling molecule FGF8. Science **294,** 1071, 2001.
73. Perrier, A.L., Tabar, V., Barberi, T., Rubio, M.E., Bruses, J., Topf, N., *et al.* Derivation of midbrain dopamine neurons from human embryonic stem cells. Proc Natl Acad Sci U S A **101,** 12543, 2004.
74. Yan, Y., Yang, D., Zarnowska, E.D., Du, Z., Werbel, B., Valliere, C., *et al.* Directed differentiation of dopaminergic neuronal subtypes from human embryonic stem cells. Stem Cells **23,** 781, 2005.
75. Nakamura, K., Mieda, T., Suto, N., Matsuura, S., and Hirai, H. Mesenchymal stem cells as a potential therapeutic tool for spinocerebellar ataxia. Cerebellum **14,** 165, 2015.
76. Chang, Y.-K., Chen, M.-H., Chiang, Y.-H., Chen, Y.-F., Ma, W.-H., Tseng, C.-Y., *et al.* Mesenchymal stem cell transplantation ameliorates motor function deterioration of spinocerebellar ataxia by rescuing cerebellar Purkinje cells. J Biomed Sci **18,** 54, 2011.
77. Song, L., Tsai, A., Yuan, X., Bejoy, J., Sart, S., Ma, T., *et al.* Neural differentiation of spheroids derived from human induced pluripotent stem cells-mesenchymal stem cells coculture. Tissue Eng Part A **24,** 915, 2018.
78. Matsuura, S., Shuvaev, A.N., Iizuka, A., Nakamura, K., and Hirai, H. Mesenchymal stem cells ameliorate cerebellar pathology in a mouse model of spinocerebellar ataxia type 1. Cerebellum **13,** 323, 2014.
79. Jin, J.-L., Liu, Z., Lu, Z.-J., Guan, D.-N., Wang, C., Chen, Z.-B., *et al.* Safety and efficacy of umbilical cord mesenchymal stem cell therapy in hereditary spinocerebellar ataxia. Curr Neurovasc Res **10,** 11, 2013.
80. Dongmei, H., Jing, L., Mei, X., Ling, Z., Hongmin, Y., Zhidong, W., *et al.* Clinical analysis of the treatment of spinocerebellar ataxia and multiple system atrophy-cerebellar type with umbilical cord mesenchymal stromal cells. Cytotherapy **13,** 913, 2011.
81. Olson, S.D., Pollock, K., Kambal, A., Cary, W., Mitchell, G.-M., Tempkin, J., *et al.* Genetically engineered mesenchymal stem cells as a proposed therapeutic for Huntington's disease. Mol Neurobiol **45,** 87, 2012.
82. Zhang, M.-J., Sun, J.-J., Qian, L., Liu, Z., Zhang, Z., Cao, W., *et al.* Human umbilical mesenchymal stem cells enhance the expression of neurotrophic factors and protect ataxic mice. Brain Res **1402,** 122, 2011.
83. Aizman, I., Tate, C.C., McGrogan, M., and Case, C.C. Extracellular matrix produced by bone marrow stromal cells and by their derivative, SB623 cells, supports neural cell growth. J Neurosci Res **87,** 3198, 2009.
84. Meyerrose, T., Olson, S., Pontow, S., Kalomoiris, S., Jung, Y., Annett, G., *et al.* Mesenchymal stem cells for the sustained *in vivo* delivery of bioactive factors. Adv Drug Deliv Rev **62,** 1167, 2010.

Address correspondence to:
Yan Li, PhD
Department of Chemical and Biomedical Engineering
FAMU-FSU College of Engineering
Florida State University
2525 Pottsdamer Street
Tallahassee, FL 32310
USA

E-mail: yli4@fsu.edu

Qing-Xiang Amy Sang, PhD
Department of Chemistry and Biochemistry
Florida State University
102 Varsity Way
Tallahassee, FL 32306
USA

E-mail: qsang@fsu.edu

Received: May 26, 2020
Accepted: August 28, 2020
Online Publication Date: October 1, 2020